J. Synchrotron Rad. (1999). **6**, 152–154

Sequence estimation of piled-up pulses in synchrotron-based XAFS

P.J. Pietraski[a,b], P. Voltz[b], L.R. Furenlid[a]

[a] *Brookhaven National Laboratory, Upton, NY 11973, USA*
[b] *Polytechnic University, Farmingdale, NY 11754, USA*

Signal processing techniques are being developed that allow XAFS and diffraction experiments employing solid state detectors to be carried out at higher count rates by resolving shaper pulses that would otherwise be rejected or corrupted due to pile-up. This method exploits the time structure of the synchrotron generated radiation and *a priori* knowledge of the incident and fluorescence energies to perform sequence of event estimation based on periodically sampled observations of the shaper amplifier output. Isolated pulses are processed with a simple threshold decision much like an SCA while non-isolated pulses that produce sequence segments of finite length are processed as vectors. Once the vector is estimated, the number of fluorescence and scatter events is counted.

Since these piled-up pulses are not rejected, the over all count rate of the experiment is increased.

Keywords: Pile-up; Time structure; Detectors; Inter-pulse Interference

1. Introduction

In most spectroscopic synchrotron based experiments, the radiation source (synchrotron radiation) is treated as a continuous source instead of a low duty cycle modulated source. While making this approximation does not usually lead to erroneous results, the time structure of synchrotron radiation can be exploited to increase the photon count rate.

Since both the bunch length and the delay from absorption to fluorescence are small compared to practical shaping times, both scatter and fluorescence events can be considered discretized and synchronized to the bunch period. With knowledge of when all the shaper pulse peaks may occur, the shaper output can be peak sampled simply by synchronizing an A/D converter to the bunch frequency, with an appropriate delay, to generate a data stream sequence. The sequence of data generated by the A/D converter represents the periodically sampled shaper output signal and contains all the shaper pulse peak values in addition to all the shaper output values when pulses were permitted to peak but did not. Because all events are forced to be separated in time by an integer multiple of the bunch period, the inter-pulse interference seen at the shaper peak sampling circuit takes on a countable number of possible values. If, in addition, the infinite impulse response (IIR) shaping amplifier is approximated as one with finite support or, a finite impulse response (FIR) filter is used, then the inter-pulse interference can take on only a finite number of possible values. Fig.1 shows a set of two photon pile-up possibilities observed with a 750nSec. six pole Gaussian shaper (Pullia, A., 1996) on X-19A during single bunch operation at the NSLS. The

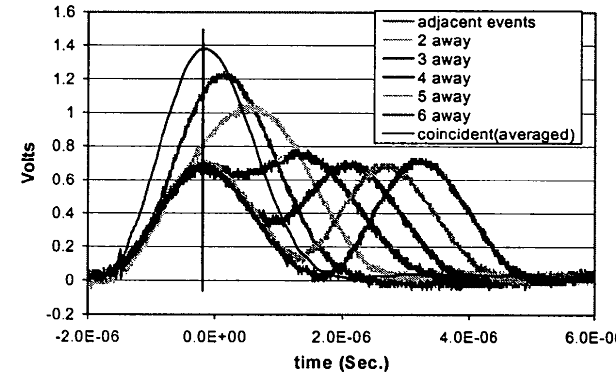

Figure 1
Superposition of the first seven 2-pulse monochromatic pile-up events observed at the output of the shaping amplifier. The shaping amplifier is six pole Gaussian, with shaping time ~750 nS. The bunch period is 568 nS. The vertical line indicates the first sample location on all the pulses. Note that sampling does not necessarily occur on the pulse peaks.

effect of this discrete set of possible pile-up possibilities is shown in the simulated MCA of fig.2. An MCA generated by a continuous source at the same count rate is superimposed for reference.

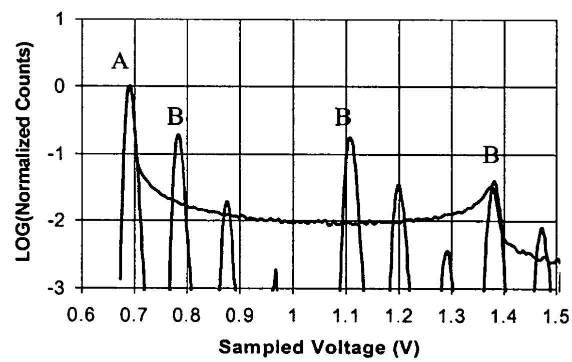

Figure 2
Simulated Log MCA of high count rate monochromatic events produced by a continuous and pulsed radiation source. The shaping amplifier is Gaussian, with shaping time ~750 nS. The bunch period is 568 nS for the pulsed source and the average photon frequency is 176KHz. MCA sampling is triggered by a fast channel signal. In the pulsed source MCA, only discrete sample values are possible (to within Fano uncertainty). The peak labeled A is produced by isolated pulses. The peaks labeled B are produced by two interfering pulses. The other peaks are formed by three or more interfering pulses.

As the count rate goes up, the performance of systems without any pile-up rejection, e.g. systems that simply sample the shaper output on all fast channel triggers, degrades quickly because all pulses corrupted by pile-up are included in generating a statistic. In order to avoid this problem, pile-up rejection of some type is typically employed. Only pulses that have negligible inter-pulse interference are used. This is accomplished by imposing a 'dead time' on the counting electronics that stops interfering pulses from being categorized and counted. The actual count rate of different energy pulses is then inferred by 'dead time correction'. (Note that in XAFS this is roughly equivalent to normalizing fluorescence to scatter.) This method works well as long as the isolated pulses make up a strong majority of the total pulses. As count rates become higher, the ratio of observed events to total events becomes smaller and at some point the frequency of observations becomes a decreasing function of photon frequency. This is because most of the events are no longer isolated but rather are part of a sequence segment of several interfering pulses.

Here we propose a method that uses *a priori* knowledge of the fluorescence energies, the scatter energy, and the time structure of the incident radiation to recover information that would otherwise be lost in sequences of interfering pulses.

2. Sequence Processing Algorithm

The first step in the algorithm is analyzing the sequence to identify the sequence segments that consist of interfering pulses, and their lengths, in the data steam generated by the A/D converter that is sampling the shaper output at the bunch frequency. In the case of uni-modal pulses, this can be accomplished without a fast channel trigger by comparing the A/D data to a threshold value that satisfies the following two conditions: 1) The level must be high enough so any set of pulses that exhibit interference small enough that they are considered isolated, have one data point between each pair of them that is below the threshold level. 2) The level must be low enough so that all data points between consecutive pulses that exhibit interference large enough that they are considered not isolated, are above the level. The amount of acceptable interference will depend on the specific application. The number of consecutive data points above the threshold level, combined with knowledge of the shaper impulse response, is then sufficient to identify isolated pulses and the lengths of the interfering pulse segments. For non-unimodal pulses, e.g. bi-polar shaper pulses, a more complicated analysis of the data stream, or the presence of a fast channel, is required.

Isolated pulses are simplest to process. Since they exhibit negligible interference, we may simply compare the peak-sampled value of the isolated pulse to a list of intervals to see which interval the sample falls into. The intervals represent the decision rule for the isolated observation. There is one simply connected interval for each energy in the photon spectrum and possibly other intervals to cover coincident events. Without knowledge of the *a priori* probabilities of the different types of events, the interval boundaries should be selected such that the decision rule selects the event that most likely produced the sample value, i.e. maximum likelihood (ML) detection (Van Trees, Harry L., 1968). This is equivalent to the pile-up rejection system with an SCA for each energy in the spectrum where the SCA window levels are optimized to produce ML results.

The segments of non-isolated pulse data require a more complicated detector but the idea is similar. Again we are interested in making a ML detector but with some compilations. The detector will operate on vectors (the data in the sequence segment of non-isolated pulses) instead of scalars (the peak value of the sequence segments of isolated pulses), and both the signal and noise components of the observations are correlated. Once the most likely vector is estimated, the number of events of each of the possible energies is counted and stored. Because the detector will now be operating on vectors, the decision rule space will be N dimensional (R^N) where N is the length of the vector being processed. This implies that the ML detector will select the most likely vector from a set of E^N possible vectors were E is the number of possible energies in the spectrum plus one. Segments of different length will be processed with different detectors in order to minimize computation. Additional information about the vector is often available (especially if a fast channel output is available) that can reduce the size of the decision space, such as knowledge of the locations within a vector where an event occurred, but the details are omitted here. Even with this possible reduction in the decision space size, vectors over a certain length will not be processed in the interest of reducing computation even though in principle vectors of any finite length may be processed.

After an observation vector of length N is extracted from the A/D data stream, the ML detector for vectors of length N is applied and the length N estimate vector is generated. The ML estimate vector is given by the formula below. The derivation will be presented elsewhere.

$$\hat{\underset{\sim}{x}} = \arg\left\{\max_{\underset{\sim}{x}\in X}\left[\left|C_x + R\right|^{-1/2}\exp\left\{-\frac{1}{2}\left(\underset{\sim}{y}^T - \underset{\sim}{\eta}_x^T\right)\left(C_x + R\right)^{-1}\left(\underset{\sim}{y} - \underset{\sim}{\eta}_x\right)\right\}\right]\right\} \quad (1)$$

Where R is the noise covariance matrix:

$$R_{m,n} = E\left\{y_n y_m \mid \underset{\sim}{x} = \underset{\sim}{0}\right\} \quad (2)$$

C is the conditional signal covariance matrix:

$$C_{x\,m,n} = E\left\{y_n y_m \mid \underset{\sim}{x}\right\} - E\left\{y_n \mid \underset{\sim}{x}\right\}E\left\{y_n \mid \underset{\sim}{x}\right\}, \quad (3)$$

η is the conditional observation mean vector:

$$\underset{\sim}{\eta}_x = E\left\{\underset{\sim}{y} \mid \underset{\sim}{x}\right\}, \quad (4)$$

X is the set of all possible N length input (photon) sequences, $\underset{\sim}{y}$ is the observation vector, and $\hat{\underset{\sim}{x}}$ is the ML vector estimate of $\underset{\sim}{x}$. If we make some assumptions about the noise matrix R, then the equation (1) may be approximated by with the much simpler one below.

$$\hat{\underset{\sim}{x}} \approx \arg\left\{\max_{\underset{\sim}{x}\in X}\left\|\underset{\sim}{y}^T T - \underset{\sim}{\eta}_x^T T\right\|_2^2\right\} \quad (5)$$

Where T is the Cholesky triangular matrix decomposition of R^{-1} (Lancaster, P., Tismenetsky, M., 1985).

The approximate ML detector in (5) requires much less computation and memory to implement and does not exhibit a substantial degradation in performance under reasonable circumstances.

2.1 *Limitations*

It should be noted that certain types of coincident events would not be resolvable. If the sum of the energy of a set of coincident photons is the same (or close) to the sum of the energy of a different set of photon(s), then these two types of events will be indistinguishable. E.g. If the sum of the energy of two fluorescence photons equals the energy of the scatter photon, they will produce the same amount of charge and be indistinguishable.

Another limitation is observed when the bunch period becomes much smaller than the shaper pulse support. In this case, the required maximum vector length to achieve a reasonable performance increase grows. This in turn requires a much larger memory and the presence of a fast channel to keep computation time reasonable.

3. Simulation Results

The detectors in (1) and (5) were both tested with realistic simulated data. Because the results of (1) and (5) were similar and the computational burden so much less than in (1), the results presented here will be for the detector in (5) only.

The data was generated to simulate a Si detector system with noise dominated by the series and parallel white noises of the Si pad and pre-amp. The shaper amplifier is taken to be the 'optimum' linear time invariant (LTI) filter, the infinite cusp filter matched to the detector/pre-amp noise (Radeka, V., 1988). The infinite cusp filter was selected both for its theoretical importance and for ease of simulation. The simulation assumes the following parameters: 1) the bunch frequency is 1.76MHz (This is the NSLS X-Ray ring single bunch frequency, f_m.) 2) The cusp filter shaping time is set to 0.8uSec. 3) The RMS equivalent noise charge is set to 30 e^-.

The data is generated such that, in each sequence to be processed, the total number of scatter photons and fluorescence photons is known and fixed and each photon generates a charge predicted by the Fano statistics (Knoll, Glenn F., 1989). Noise with the appropriate auto-correlation properties is also added. The number of scatter (7800eV) photons, N_s, is 200 and the number of fluorescence (7200eV) photons, N_f, is 100 in each analyzed sequence. The average photon frequency, f_p, is controlled by changing the total length of the sequence while keeping N_s and N_f fixed. The detector performance for several maximum vector lengths is compared against the pile-up reject detector, i.e. processing only the isolated pulses. The performance of the detectors is measured by: 1) comparing their observed photon frequency, f_{op}, Vs actual photon frequency, f_p and 2) by comparing the variance of the estimate of the ratio of the number of fluorescence photons to scatter photons, N_f/N_s of the different detectors. This is done for vector length maximums of N=3,4,5,6 and for the isolated pulses (N=1). As can be seen in figure 3, the observed count rates for the pile-up reject detector has a maximum of about $0.04f_m$ while that of the N=5 ML detector achieves about double the count rate at its maximum. This is reflected in the variance of the estimate of N_f/N_s. Figure 4 shows that the variance of the estimate made by the ML detectors is superior to that of the pile-up reject detector.

4. Conclusions

A sequence processing algorithm has been described that permits faster categorization and counting of photons in synchrotron based spectroscopy. This is accomplished by recovering data that would normally be discarded because pile-up had caused too much interference. This increase in count rate leads to experimental data with smaller variance and/or permits experiments to be conducted in a shorter period of time.

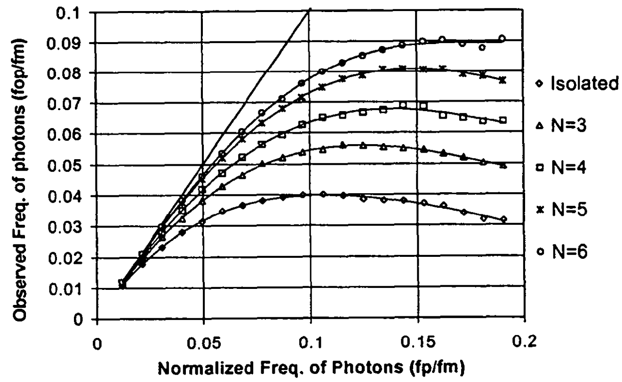

Figure 3
Observed count rates for detectors capable of processing vectors of length 1 through 6 normalized to the bunch frequency. A line of slope one is given for reference.

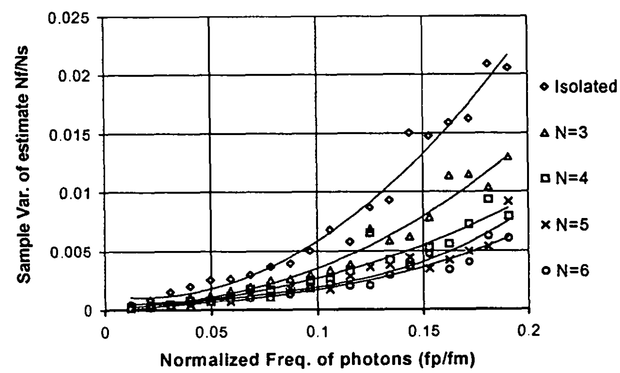

Figure 4
Sample variance of the estimate N_f/N_s for detectors capable of processing vectors of length one through six for a fixed number of fluorescence and scatter photons vs. incident photon frequency normalized to the bunch frequency.

5. Acknowledgements

We would like to thank Roger Klaffky for arranging single bunch operations time on the NSLS X-Ray ring.

The NSLS is operated by Brokhaven National Laboratory under contract DE-AC02-76CH00016 with the U.S. Department of Energy, Office of Basic Energy Science.

References

Knoll, Glenn F., 2nd Ed. John Wiley and Sons, Inc., New York, NY, 1989

Lancaster, P., Tismenetsky, M., Academic Press, San Diego, CA 1985

Pullia, A., Furenlid, L., Kraner, H.W., Bertuccio, G., Pietraski, P. J., Siddons, D. P., Rev. Sci. Inst., (1996) 67,9,1-8

Radeka, V., Annual Review of Nuclear Science 38, (1988) 211-277

Van Trees, Harry L., John Wiley and Sons, Inc., New York, NY, 1968

(Received 10 August 1998; accepted 6 November 1998)